J. Fluid Mech. (1998), *vol.* 364, *pp.* 273–295. Printed in the United Kingdom

Stability of vapour–liquid counterflow in porous media

By IRENE PESTOV

Department of Mathematics, Victoria University of Wellington, Wellington, NZ

(Received 14 November 1996 and in revised form 29 January 1998)

A linear stability analysis of vapour–liquid counterflow in porous media is carried out. For the vapour-dominated basic state the development in time of both pressure and saturation disturbances is studied. The pressure field is shown to be asymptotically stable for all choices of thermal boundary conditions, excluding the insulating–insulating boundary condition for which it is neutrally stable. The saturation field is proven to be Lyapunov stable: the saturation disturbance remains bounded by an infinitesimal number at all times. For both vapour- and liquid-dominated basic states the direction of propagation of small saturation disturbances is determined. These results explain the formation of two-layer geothermal structures and why alternative structures cannot develop within homogeneous reservoirs.

1. Introduction

Vapour–liquid counterflow occurs naturally in geothermal reservoirs: vapour flows upward and the condensate moves downward with the net mass flux remaining very small (White, Muffler & Truesdell 1971). Vapour–liquid counterflow can be either vapour- or liquid-dominated. In the vapour-dominated counterflow vapour is the most mobile phase, and in the liquid-dominated counterflow liquid is the most mobile phase.

The existence of vapour–liquid counterflow is supported by field measurements. Nearly isothermal temperature distributions and small pressure gradients, which exceed the vapour-static pressure gradient only slightly, have been recorded in the upper parts of the Geysers geothermal field in California (Thomas *et al.* 1981), Larderello in Italy (Pruess *et al.* 1987), and Wairakei in New Zealand (Allis & Hunt 1986). Such regions are modelled as vapour-dominated counterflowing zones. Larger temperature and pressure gradients, typical of liquid-dominated counterflow, are found in the lower parts of Larderello (Pruess *et al.* 1987). The flow in the lower parts of the Geysers and Wairakei reservoirs is also characterized by larger temperature gradients (Drenick 1986; Walters *et al.* 1988; Allis & Hunt 1986). These temperature gradients, however, cannot be accommodated into a vapour–liquid counterflow model. In all three reservoirs an increase in temperature gradients is abrupt, which clearly indicates the presence of two superposed layers saturated by water and steam in different proportions. Most intriguing, there is no drilling evidence of low permeability barriers or permeability contrasts between the upper and lower layers.

These observation results have been reflected in the following conceptual models.

Model A: a vapour-dominated zone over a water region (White *et al.* 1971).

Model B: a vapour-dominated zone over a steam region (Truesdell 1991).

Model C: a vapour-dominated zone over a liquid-dominated zone (Pruess *et al.* 1987).

Models A and B are appropriate for some parts of the Wairakei and Geysers geothermal fields respectively, and model C accommodates the Larderello observations.

In addition we shall consider here another two-layer model.

Model D: a water layer over a liquid-dominated region.

This structure was first obtained in laboratory experiments by Bau & Torrance (1982) and later derived from theoretical considerations by Pestov (1997). To date there is no clear field evidence that such a structure could develop in nature, although the Kawah Kamojang geothermal field in Indonesia resembles some of its features.

Structured geothermal systems have been of significant interest in geothermal modelling. This interest dates back to the linear stability work of Schubert & Straus (1980), who studied the gravitational stability of superposed layers of water and steam in porous media. Their approach was extended by including the effects of vapour–liquid counterflow in the analytical and numerical works of Ramesh & Torrance (1990, 1993). In these papers, however, an underlying counterflowing region was assumed to be isothermal, and only pressure disturbances were considered. (Two-phase counterflow is not isothermal, and the development in time of saturation disturbances is equally important, as we shall show further.) Weir & Young (1991) and Kissling *et al.* (1992) investigated the propagation of saturation discontinuities in porous media saturated by water and steam. Their numerical experiments led to a better understanding of flows in two-phase regions. The evolution of structured reservoirs has been modelled in computer experiments. Shook (1993) was the first to obtain on a computer the controversial Geysers model (structure B). Lai, Bodvarsson & Truesdell (1994) simulated structures similar to A, B and C. There have been numerous studies on steady heat and mass transfer in geothermal systems. McGuinness (1996) examined two-phase steady-state solutions in a temperature-saturation plane with capillary effects included, and determined which solution (vapour- or liquid-dominated) is likely to occur in actuality. Young (1996) investigated phase transitions in vertical hydrothermal flow using entropy and thermodynamic inequalities at the phase boundary. These results, although restricted to steady one-dimensional flows, are fully supported by the present linear stability analysis.

In this paper the formation of different two-layer structures within homogeneous reservoirs is explained using the quasi-static approximation for geothermal processes. In Appendix A we illustrate how a real geothermal process can be approximated by a quasi-static path. Since a quasi-static process is a series of transitions between neighbouring equilibrium states (steady-states), it is important to know that all these states are stable. In the next section we consider the stability of vapour-dominated counterflow. This case is particularly important in geothermal modelling since the observed structures A, B and C contain a vapour-dominated counterflowing region. The liquid-dominated case is too complicated for analytical studies and must be treated numerically. It is, however, possible to find the direction of propagation of small saturation disturbances for both vapour- and liquid-dominated cases. The direction in which small saturation waves propagate is determined by the sign of the saturation wave speed in the linearized saturation equation. In § 2.2 and Appendix C we give explicit analytical expressions for the wave speed in vapour- and liquid-dominated media respectively. Another important question we address in the next section is related to the relaxation time to restore thermodynamic equilibrium. It

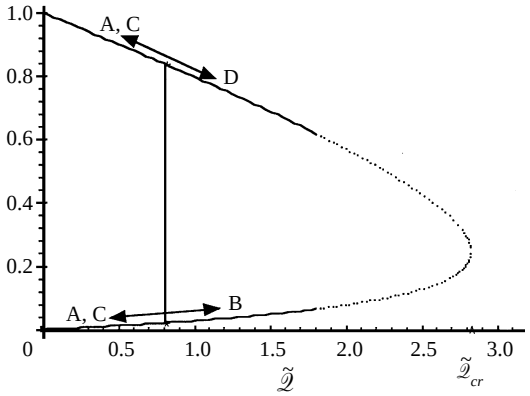

FIGURE 1. Liquid relative permeability versus $\tilde{\mathcal{Q}}$.

must be taken into account that the process of returning to equilibrium is not instantaneous. This will help to explain why the alternative inverse structures IA (a water region above), IB (a steam layer above), IC (a liquid-dominated zone over a vapour-dominated region), and ID (a water layer below) cannot develop within a homogeneous reservoir.

In our earlier work (Pestov 1995) we conjectured that the following geothermal processes may lead to the formation of the two-layer structures:

- a decrease/increase in the heat flux Q at the reservoir lower boundary;
- a decrease/increase in reservoir vertical permeability k;
- the injection/withdrawal of fluid through reservoir boundaries.

The heat flux Q may decrease or increase in response to changes in igneous activity. Permeability k may vary in response to deposition/dissolution of chemicals and rock compression. In the non-dimensional governing equations these changes are represented through the dimensionless heat flux $\tilde{\mathcal{Q}}$ (Pestov 1997):

$$\tilde{\mathcal{Q}} = \frac{\mu_l^* Q}{\tilde{m} k \rho_l^* g \rho_l^* l^*}. \tag{1.1}$$

Here and in the following, the symbol $\sim$ marks values at the upper boundary (cooler surface), the superscript $*$ denotes characteristic quantities, the subscripts v and l indicate the vapour and liquid phase respectively, $\mu_{l,v}$ are dynamic viscosities, $\rho_{l,v}$ are densities, g is the acceleration due to gravity, l is latent heat, and $\tilde{m}$ is the ratio between the vapour and liquid phase densities calculated at the upper boundary. The dimensionless heat flux $\tilde{\mathcal{Q}}$ is the key parameter which governs the phase distribution inside a two-phase zone. The first two processes (changes in Q and k) affect the phase distribution within a two-phase zone whereas the last processes (injection/withdrawal of fluid) change its vertical extent.

With the quasi-static approximation the evolution of a geothermal system can be modelled using the steady-state solutions. Figure 1 presents steady-state liquid relative permeability k_{rl} calculated at the upper boundary as a function of $\tilde{\mathcal{Q}}$. The temperature at the upper boundary $\tilde{T}$ is taken to be 513 K, effective thermal conductivity α is $3.2\,\mathrm{W\,m^{-1}\,K^{-1}}$, and permeability k is $10^{-14}\,\mathrm{m^2}$, values typical of the Geysers geothermal field. The upper and lower branches represent liquid- and vapour-dominated solutions respectively. $\tilde{\mathcal{Q}}^{cr}$ is the upper bound for the existence of vapour–liquid counterflow in porous media (Pestov 1994). There are also two lower bounds according

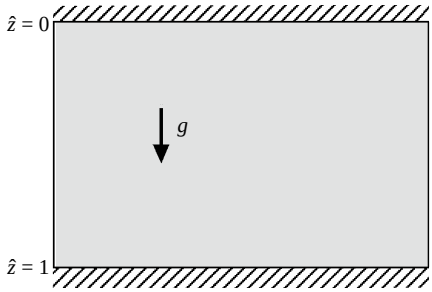

FIGURE 2. Sketch of a porous medium saturated by water and steam.

to McGuinness & Pestov (1996). The lower bounds cannot be seen in figure 1 since they are very small for the range of parameters which apply to the Geysers geothermal field. The possible ways that lead to different two-layer structures are shown by arrows. The initial states are taken to be fully two-phase (shown by asterisks at the lower and upper branches). Curves denote the quasi-static changes in $\tilde{\mathcal{Q}}$ when the total amount of water inside a reservoir is held fixed (impermeable boundaries). The vertical line represents a quasi-static injection/withdrawal process connecting the initial states ($\tilde{\mathcal{Q}}$ is held fixed). Structures A and C may develop from both liquid- and vapour-dominated initial states when $\tilde{\mathcal{Q}}$ is decreasing and the total amount of water is held fixed. Which of two possibilities is realized is determined by the lower bound for the existence of liquid-dominated counterflow in porous media (McGuinness & Pestov 1996). When $\tilde{\mathcal{Q}}$ is increasing and the total amount of water is held fixed, either structure B or structure D may be formed depending on the initial state of a reservoir. If the initial state is vapour-dominated, then structure B develops (see the lower branch in figure 1). If the initial state is liquid-dominated, then structure D develops (see the upper branch in figure 1).

In what follows, we analyse the sensitivity of vapour-dominated counterflow to small disturbances. For our purposes, it is satisfactory to assume that either the equilibrium between liquid and vapour phases is not affected by the processes considered, or that the relaxation time to restore the equilibrium between phases is much less than the time to return to the state of mechanical equilibrium.

2. Linear stability analysis

Consider a porous medium saturated by a two-phase water–steam mixture and bounded by two parallel planes at $\hat{z} = 0$ and $\hat{z} = 1$ as sketched in figure 2. (Here $\hat{z}$ is the dimensionless vertical coordinate pointing in the direction of gravity.) We assume that there is no external force acting in the horizontal direction, and that hydrodynamic and thermal boundary conditions are uniform (e.g. either a constant temperature or a constant heat flux is prescribed at the boundary). In addition we assume that

- capillary pressure is unimportant;
- conduction is negligible;
- vapour enthalpy and latent heat variations can be neglected;
- liquid phase density can be taken as constant.

The validity of these assumptions for two-phase geothermal reservoirs has been confirmed by numerous analytical and computer studies (see, for example, Cheng 1978; O'Sullivan, Zyvoloski & Blakeley 1983; McGuinness *et al.* 1993; Pestov 1997).

The first assumption is often used in analytical studies. While capillary pressure is important for capillary-driven counterflow, it can be ignored in a geothermal reservoir where the liquid-phase motion is caused by gravity (Schubert & Straus 1980; Ramesh & Torrance 1990). In the non-dimensional governing equations the capillary pressure effects are represented by the dimensionless ratio $\sigma\bar{r}/\mu^* V^* L^*$ (Barenblatt, Entov & Ryzhik 1990). Here σ is interfacial tension for water and steam, $\bar{r}$ is mean radius of curvature of the interface at the pore level, V^* is characteristic velocity, μ^* is characteristic dynamic viscosity, and L^* is characteristic length. For a typical geothermal reservoir this ratio is much less than 1 (Pestov 1997). This assumption, however, does not hold in the interfacial layers where rapid changes in saturation occur (McGuinness 1996).

The second assumption is generally accepted for vapour-dominated reservoirs. It is also valid for high-permeability liquid-dominated reservoirs with high vertical heat fluxes (McGuinness & Pestov 1996; McGuinness 1997).

The last two assumptions are satisfied in most practical situations except for two-phase zones with vertical temperature gradients of the order of 100 K and with bottom temperatures higher than 330 °C (Pestov 1997). The assumption of constant liquid-phase density emphasizes the physical fact that the main driving mechanism in two-phase flow is the difference between the phase densities.

The macroscopic conservation equations for the flow in a two-phase geothermal reservoir are well presented in the geothermal literature (cf. Garg & Pritchett 1977; Cheng 1978). With the above assumptions a non-dimensional form of these equations is (Pestov 1997)

continuity equation

$$\frac{\partial\,(\tilde{m}\varphi S_v + S_l)}{\partial \hat{t}} + \hat{\nabla}\cdot(\boldsymbol{J}_v + \boldsymbol{J}_l) = 0, \tag{2.1}$$

energy equation (*two equivalent forms*)

$$\frac{\sigma\tilde{\delta}\epsilon}{\phi}\varphi^{\epsilon-1}\,\bar{p}\,\frac{\partial \hat{p}}{\partial \hat{t}} + \hat{l}\left[\partial(\tilde{m}\varphi S_v)/\partial\hat{t} + \hat{\nabla}\cdot(\boldsymbol{J}_v)\right] = 0, \tag{2.2}$$

$$\frac{\sigma\tilde{\delta}\epsilon}{\phi}\varphi^{\epsilon-1}\,\bar{p}\,\frac{\partial \hat{p}}{\partial \hat{t}} - \hat{l}\left[\partial S_l/\partial\hat{t} + \hat{\nabla}\cdot(\boldsymbol{J}_l)\right] = 0. \tag{2.3}$$

Here $S_{v,l}$ are saturations, $k_{rv,l}$ are relative permeabilities, $\varphi = p/\tilde{p} = \bar{p}\hat{p} + 1$, p is pressure, $\hat{p}$ is dimensionless pressure normalized by the vertical pressure difference p^*, $\bar{p} = p^*/\tilde{p}$ is the pressure jump, $\hat{l}$ is non-dimensional latent heat normalized by its value l^* at $\hat{z} = 0$, ϕ is porosity, $\hat{t} = t/t^*$ is dimensionless time, and t^* is a characteristic time scale defined as the ratio of the vertical distance H to the characteristic velocity of a liquid particle (Pestov 1997). All distances are normalized by H. Vectors $\boldsymbol{J}_v$ and $\boldsymbol{J}_l$ can be interpreted as the dimensionless mass flux densities of the vapour and liquid phase respectively. When Darcy's law is assumed, the corresponding expressions are

$$\boldsymbol{J}_v = -\frac{k_{rv}\varphi}{\mu\tilde{\mathscr{Q}}}\left(\gamma\hat{\nabla}\hat{p} - \tilde{m}\varphi\boldsymbol{e}_z\right), \tag{2.4}$$

$$\boldsymbol{J}_l = -\frac{k_{rl}}{\tilde{m}\tilde{\mathscr{Q}}}\left(\gamma\hat{\nabla}\hat{p} - \boldsymbol{e}_z\right), \tag{2.5}$$

where $\boldsymbol{e}_z$ is a unit vector in the direction of gravity.

Two equivalent forms (2.2) and (2.3) are obtained by combining the energy equation with the continuity equation.

Equations (2.1)–(2.3) involve the following non-dimensional parameters (Pestov 1997): μ is the ratio of the dynamic viscosity of steam to that of water (taken as constant), $\gamma = p^*/\rho_l^* gH$ is the ratio of the characteristic pressure difference to the liquid-static pressure difference, σ is the heat capacity ratio of saturated rock to that of water (taken as constant), $\tilde{\delta} = C_{pl}\tilde{T}/l^*$ and $\epsilon = c/l^*$ are latent heat factors. Parameter $\tilde{\delta}$ involves the specific heat of water at constant pressure C_{pl}. Parameter ϵ involves the constant c from the following state equation for the vapour phase:

$$p/\rho_v = c = \text{const.} \tag{2.6}$$

Equation (2.6) emphasizes the empirical fact that in a two-phase flow the saturated vapour density, ρ_v, varies with temperature (and, hence, with depth), whereas the ratio between ρ_v and the saturation pressure remains constant. Equation (2.6) gives better results than the ideal gas approximation for high temperatures and pressures, which are often the case in practical applications, e.g. in a geothermal reservoir (Pestov 1994).

Another analytical approximation used in equations (2.1)–(2.3) is the power fit obtained in our earlier work (Pestov 1994):

$$\frac{T}{\tilde{T}} = \left(\frac{p}{\tilde{p}}\right)^{\epsilon}. \tag{2.7}$$

The power fit (2.7) gives a better match to the Clausius–Clapeyron equation compared to the other approximations in the temperature range of 200–300 °C typical of two-phase reservoirs. According to the dimensional analysis results given in Pestov (1997), only minor features of the flow are neglected in equations (2.1)–(2.3).

Equations (2.1)–(2.3) must be solved together with hydrodynamic and thermal boundary conditions. We take both boundaries, $\hat{z} = 0$ and $\hat{z} = 1$, to be impermeable and prescribe either constant temperatures at both boundaries (*conducting–conducting boundary condition*), or a constant temperature at one boundary and a constant heat flux at the other boundary (*conducting–insulating boundary condition*), or a constant heat flux at both boundaries (*insulating–insulating boundary condition*). (Here we follow the terminology pertaining to the Rayleigh–Bénard problem.) Since relative permeabilities and saturations are functionally dependent (Bear & Bachmat 1991), we take $k_{rl} = \psi(S_l)$ and $k_{rv} = 1 - \psi(S_l)$, where ψ is some relative permeability function of a general form. Then, with the help of (2.7), the whole problem can be reduced to two dependent variables, e.g. saturation pressure and one of the relative permeabilities.

Decompose now the dependent variables into unperturbed (superscript zero) and perturbed (superscript prime) quantities:

$$p(x, y, z, t) = p^{\circ}(z) + o\,p'(x, y, z, t),$$

$$k_{rl}(x, y, z, t) = k_{rl}^{\circ}(z) + o\,k'(x, y, z, t) = \psi(S_l^{\circ} + o\,S').$$

(Here and in the following 'hats' for non-dimensional quantities are dropped.)

Let us take the one-dimensional steady vapour-dominated solution (the lower branch in figure 1) as the basic unperturbed state. Although a simplification of reality, this solution describes the heat and mass transfer processes in many two-phase geothermal reservoirs. For the range of parameters in which some two-phase systems operate (e.g. the Geysers and Wairakei systems), this solution seems to be the only one possible (McGuinness & Pestov 1996).

After substituting perturbed dependent variables into (2.1)–(2.3) and neglecting second- and higher-order small quantities we obtain the following linearized equations:

continuity equation

$$(1-\underbrace{\tilde{m}\varphi^{\circ}}_{O(\tilde{m})})\frac{\partial S'}{\partial t}+c_l\left(1+\underbrace{\frac{c_v}{c_l}\varphi^{\circ}}_{O(\tilde{m}\tilde{\mathcal{Q}})}\right)\frac{\partial k'}{\partial z}=\frac{\overline{p}}{\overline{p}_{ls}\mu\tilde{\mathcal{Q}}}\Phi_v+\frac{\overline{p}}{\overline{p}_{ls}\tilde{m}\tilde{\mathcal{Q}}}\Phi_l, \tag{2.8}$$

energy equation (*two equivalent forms*)

$$-\tilde{m}\varphi^{\circ}\frac{\partial S'}{\partial t}+c_v\,\varphi^{\circ}\frac{\partial k'}{\partial z}=\frac{\overline{p}}{\overline{p}_{ls}\mu\tilde{\mathcal{Q}}}\Phi_v[p'], \tag{2.9}$$

$$\frac{\partial S'}{\partial t}+c_l\frac{\partial k'}{\partial z}=\frac{\overline{p}}{\overline{p}_{ls}\tilde{m}\tilde{\mathcal{Q}}}\Phi_l[p'], \tag{2.10}$$

where

$$\Phi_v[p']=\frac{\partial}{\partial z}\left[k_{rv}^{\circ}\,\varphi^{\circ}\left(\frac{\partial p'}{\partial z}+\frac{1}{\varphi^{\circ}}\frac{\mathrm{d}\varphi^{\circ}}{\mathrm{d}z}\,p'-2\tilde{m}\overline{p}_{ls}\,p'\right)\right]$$
$$+k_{rv}^{\circ}\varphi^{\circ}\,\tilde{\nabla}^2\,p'-\overline{p}_{ls}\mu\tilde{\mathcal{Q}}\left[\tilde{m}\,S_v^{\circ}+v\,(\varphi^{\circ})^{\epsilon-1}\right]\frac{\partial p'}{\partial t}, \tag{2.11}$$

$$\Phi_l[p']=\frac{\partial}{\partial z}\left(k_{rl}^{\circ}\frac{\partial p'}{\partial z}\right)+k_{rl}^{\circ}\,\tilde{\nabla}^2p'+\overline{p}_{ls}\tilde{m}\tilde{\mathcal{Q}}v\;(\varphi^{\circ})^{\epsilon-1}\;\frac{\partial p'}{\partial t}, \tag{2.12}$$

$$c_v=\frac{q-\tilde{m}\varphi^{\circ}}{\mu\tilde{\mathcal{Q}}},\quad c_l=\frac{1-q}{\tilde{m}\tilde{\mathcal{Q}}}, \tag{2.13}$$

$$\tilde{\nabla}^2=\frac{\partial^2}{\partial x^2}+\frac{\partial^2}{\partial y^2},\quad q=\frac{\overline{p}}{\overline{p}_{ls}}\frac{\mathrm{d}p^{\circ}}{\mathrm{d}z},\quad v=\frac{\sigma\tilde{\delta}\epsilon}{\phi},\quad \overline{p}_{ls}=\frac{\rho_l^*gH}{\tilde{p}}. \tag{2.14}$$

Unless $\tilde{\mathcal{Q}}\sim\tilde{\mathcal{Q}}^{cr}$, for the vapour-dominated basic state we have (Pestov 1996)

$$k_{rl}^{\circ}\sim\tilde{m}\tilde{\mathcal{Q}}\ll k_{rv}^{\circ}\sim 1\Rightarrow k_{rv}^{\circ}\sim\frac{k_{rl}^{\circ}}{\tilde{m}\tilde{\mathcal{Q}}};$$

$$q\sim\tilde{m}+\mu\tilde{\mathcal{Q}}\ll 1\Rightarrow c_l\sim\frac{1}{\tilde{m}\tilde{\mathcal{Q}}}\gg c_v\varphi^{\circ}\sim 1;$$

$$q\approx\text{const}\Rightarrow\varphi^{\circ}\approx\overline{p}z+1;$$

$$k_{rv}^{\circ}\approx\text{const},\ c_l\approx\text{const},\ c_v\varphi^{\circ}\approx 1.$$

Since $\tilde{m}$ and c_v/c_l are small compared to 1, the under-braced coefficients in (2.8) can be neglected. Subtracting the resulting equation from equation (2.10) gives, as a first approximation, $\Phi_v[p']=0$. Thus, unless $\tilde{\mathcal{Q}}\sim\tilde{\mathcal{Q}}^{cr}$, the saturation disturbance and its derivatives can be eliminated from equations (2.8)–(2.10) and a single second-order equation for the pressure disturbance can be obtained for the vapour-dominated basic state. After determining the pressure disturbance, the saturation disturbance can be found from equation (2.10).

2.1. *Pressure equation*

The condition $\Phi_v[p']=0$ gives the following parabolic equation for the pressure disturbance:

$$\frac{\partial}{\partial\zeta}\left(\zeta^2\frac{\partial p'}{\partial\zeta}\right)+\zeta^2\,\tilde{\nabla}^2\,p'-\vartheta\,(\overline{p}\zeta)^{\epsilon}\frac{\partial p'}{\partial t}=0, \tag{2.15}$$

where $\vartheta = \overline{p}_{ls}\mu\tilde{\mathcal{Q}}v/(\overline{p})^2 k^{\circ}_{rv}$ and $\zeta = z + 1/\overline{p}$ is a new independent variable ($\zeta \in [\zeta_1, \zeta_2]$, $\zeta_1 = 1/\overline{p}$, $\zeta_2 = 1/\overline{p} + 1$).

We assume the solution of equation (2.15) to be of the form $p' = \exp(-\lambda t) f(x, y)\mathscr{P}(\zeta)$ provided that

$$\frac{\partial^2 f}{\partial x^2} + \frac{\partial^2 f}{\partial y^2} = -a^2 f,$$

where a is any real number. This equation is the *reduced wave equation* (Zauderer 1983), and its solution, f, can be resolved into sinusoidal components $e^{i(\chi x + \xi y)}$ of x and y. Then, $a : a^2 = \chi^2 + \xi^2$ can be interpreted as the horizontal wavenumber.

After separating variables, we can write the following equation for $\mathscr{P}$:

$$L[\mathscr{P}(\zeta)] = -\frac{\mathrm{d}}{\mathrm{d}\zeta}\left(\zeta^2 \frac{\mathrm{d}\mathscr{P}}{\mathrm{d}\zeta}\right) + a^2\zeta^2\mathscr{P} = \lambda\vartheta(\overline{p}\zeta)^{\epsilon}\mathscr{P}. \tag{2.16}$$

In the linearized form the thermal boundary conditions for $\mathscr{P}$ become

$$\left.\begin{array}{l} \alpha_1\mathscr{P}(\zeta) + \beta_1\mathscr{P}_{\zeta}(\zeta) = 0 \quad \text{at} \quad \zeta_1 = 1/\overline{p}, \\ \alpha_2\mathscr{P}(\zeta) + \beta_2\mathscr{P}_{\zeta}(\zeta) = 0 \quad \text{at} \quad \zeta_2 = 1/\overline{p} + 1. \end{array}\right\} \tag{2.17}$$

In (2.17) we set $\beta_i = 0$, $\alpha_i = 1$ when constant temperature is imposed at the boundary ζ_i, and $\beta_i = 1$, $\alpha_i = 0$ when constant heat flux is imposed at ζ_i. Thus, the conducting–conducting boundary condition will correspond to the following combination: $\beta_1 = \beta_2 = 0$ and $\alpha_1 = \alpha_2 = 1$. Setting $\beta_1 = \beta_2 = 1$ and $\alpha_1 = \alpha_2 = 0$ will give the insulating–insulating boundary condition. The conducting–insulating boundary condition will be obtained by setting $\beta_1 = 0$, $\beta_2 = 1$ and $\alpha_1 = 1$, $\alpha_2 = 0$ and vice versa.

Note that equation (2.16) together with boundary conditions (2.17) is a regular *Sturm–Liouville* problem. Indeed, $\zeta^2 > 0$, $(\overline{p}\zeta)^{\epsilon} > 0$, $a^2\zeta^2 \geqslant 0$, and these coefficients and the derivative $(\zeta^2)_{\zeta}$ are continuous in the closed interval $[\zeta_1, \zeta_2]$. The important property of a regular Sturm–Liouville problem is that the eigenvalues are all real and nonnegative, and they can be arranged in ascending order of magnitude as follows: $0 \leqslant \lambda_1 < \lambda_2 < \ldots < \lambda_n < \ldots$ (Zauderer 1983). Moreover, when $a^2 > 0$, $\lambda = 0$ cannot be an eigenvalue, and when $a^2 = 0$ (the horizontal disturbances of an infinite wavelength), $\lambda = 0$ is an eigenvalue if and only if $\alpha_1 = \alpha_2 = 0$ (insulating–insulating boundary condition) (Zauderer 1983). These results follow from the self-adjointness and positivity of the differential operator $L[\mathscr{P}(\zeta)]$. Further we shall construct the complete spectrum of the eigenvalues and the corresponding real-valued eigenfunctions of the problem stated above.

Let us introduce the new dependent variable $P(\zeta) : \mathscr{P}(\zeta) = P(\zeta)/\zeta^{1/2}$. Then (2.16) becomes

$$\zeta^2 P_{\zeta\zeta} + \zeta P_{\zeta} + \left[\lambda\vartheta(\overline{p}\zeta)^{\epsilon} - a^2\zeta^2 - \tfrac{1}{4}\right] P = 0. \tag{2.18}$$

We now show that $\lambda = 0$ is not an eigenvalue. Indeed, setting $\lambda = 0$ gives the general solution of equation (2.18) represented by elementary functions $\zeta^{1/2}$ and $\zeta^{-1/2}$ when $a = 0$ (linear horizontal disturbances), and by elementary functions $\sinh(a\zeta)/(a\zeta)^{1/2}$ and $\cosh(a\zeta)/(a\zeta)^{1/2}$ when $a > 0$ (general case). In the general case the boundary conditions (2.17) force us to choose constants $C_1 = C_2 = 0$, which leads to $P(\zeta) \equiv 0$. In the case of linear horizontal disturbances, only the insulating–insulating boundary condition gives a non-trivial solution. Thus, the complete spectrum of eigenvalues includes $\lambda = 0$ if and only if the insulating–insulating boundary condition is imposed.

2.1.1. *Infinite horizontal wavelength*

Setting $a = 0$ and introducing the new independent variable $\tilde{\zeta}^2 = 4\lambda\vartheta(\bar{p}\zeta)^\epsilon/\epsilon^2$ reduces equation (2.18), in the case of negative λ, to the *modified Bessel's* equation. The general solution of this equation is a linear combination of modified Bessel functions of real order, which are monotonic (Watson 1952). Hence, there are only trivial solutions satisfying the boundary conditions (2.17).

In the case of positive λ, equation (2.18) is *Bessel's* equation, which has non-trivial solutions (Watson 1952) satisfying the boundary conditions (2.17) (returning to the old independent variable ζ):

$$P_n = C_1 J_{1/\epsilon}\left[\frac{2}{\epsilon}(\lambda_n\vartheta)^{1/2}(\bar{p}\zeta)^{\epsilon/2}\right] + C_2 Y_{1/\epsilon}\left[\frac{2}{\epsilon}(\lambda_n\vartheta)^{1/2}(\bar{p}\zeta)^{\epsilon/2}\right]. \tag{2.19}$$

For the conducting–conducting boundary condition the eigenvalue problem reduces to finding roots of the cross-product

$$J_{1/\epsilon}(\tilde{\zeta})Y_{1/\epsilon}(b\tilde{\zeta}) - J_{1/\epsilon}(b\tilde{\zeta})Y_{1/\epsilon}(\tilde{\zeta}),$$

which has an infinite set of discrete positive roots $r_1 < r_2 < \ldots < r_n < \ldots$ (Abramowitz & Stegun 1968). The latter yields the increasing sequence of positive eigenvalues

$$\lambda_n = \frac{\bar{r}_n^2\epsilon^2 n^2\pi^2}{4\vartheta}[(1+\bar{p})^{\epsilon/2} - 1]^{-2}, \tag{2.20}$$

where

$$\bar{r}_n = \frac{r_n(b-1)}{n\pi}, \quad b = (1+\bar{p})^{\epsilon/2}$$

and $\bar{r}_n = 1 + O(n^{-2})$ for large n.

For small ϵ formulas (2.19)–(2.20) become (neglecting ϵ^2)

$$P_n = C_1 J_{1/\epsilon}\left[\frac{\bar{r}_n n\pi}{\log(1+\bar{p})}\left(\frac{2}{\epsilon} + \log(\bar{p}\zeta)\right)\right] + C_2 Y_{1/\epsilon}\left[\frac{\bar{r}_n n\pi}{\log(1+\bar{p})}\left(\frac{2}{\epsilon} + \log(\bar{p}\zeta)\right)\right], \tag{2.21}$$

$$\lambda_n = \frac{\bar{r}_n^2 n^2\pi^2}{\vartheta\log^2(1+\bar{p})}. \tag{2.22}$$

The above results can easily be extended to include the constant-heat-flux boundary condition. For the conducting–insulating thermal boundary condition the eigenvalue problem reduces to finding roots of the cross-product

$$J_{1/\epsilon}(\zeta_1)Y'_{1/\epsilon}(\zeta_2) - J'_{1/\epsilon}(\zeta_2)Y_{1/\epsilon}(\zeta_1).$$

For the insulating–insulating boundary condition we obtain the cross-product

$$J'_{1/\epsilon}(\zeta_1)Y'_{1/\epsilon}(\zeta_2) - J'_{1/\epsilon}(\zeta_2)Y'_{1/\epsilon}(\zeta_1).$$

Each cross-product has an infinite set of discrete positive roots (Abramowitz & Stegun 1968) that will yield a countable increasing sequence of positive eigenvalues λ_n.

2.1.2. *Finite horizontal wavelength*

Consider now the general case $a \neq 0$. Note that

$$(\bar{p}\zeta)^\epsilon = 1 + \epsilon\log(\bar{p}\zeta) + O(\epsilon^2) \tag{2.23}$$

unless ϵ and $|\log(\bar{p}\zeta)|$ are large, which is unlikely for vapour-dominated counterflow.

Equation (2.18) becomes

$$\zeta^2 P_{\zeta\zeta} + \zeta P_\zeta - (a^2\zeta^2 + \eta^2)P = -\lambda\vartheta\epsilon \log(\overline{p}\zeta)\, P, \tag{2.24}$$

where $\eta^2 = 1/4 - \lambda\vartheta$.

Assume the solution of equation (2.24) to be of the form

$$P = P^{(0)} + \epsilon P^{(1)} + \dots . \tag{2.25}$$

Here $P^{(0)}$ is a solution of the *modified Bessel's* equation

$$\zeta^2 P^{(0)}_{\zeta\zeta} + \zeta P^{(0)}_\zeta - (a^2\zeta^2 + \eta^2)P^{(0)} = 0 \tag{2.26}$$

with boundary conditions

$$P^{(0)}(\zeta_1) = P^{(0)}(\zeta_2) = 0, \tag{2.27}$$

$P^{(1)}$ is a solution of the non-homogeneous equation

$$\zeta^2 P^{(1)}_{\zeta\zeta} + \zeta P^{(1)}_\zeta - (a^2\zeta^2 + \eta^2)P^{(1)} = -\lambda\vartheta\epsilon \log(\overline{p}\zeta)\, P^{(0)} \tag{2.28}$$

with boundary conditions

$$P^{(1)}(\zeta_1) = P^{(1)}(\zeta_2) = 0 \tag{2.29}$$

and so on. (For the sake of definiteness, we take the conducting–conducting boundary condition.)

Note that the leading-order equation (2.26) is invariant with respect to wavenumber a (e.g. use the rescaling $\overline{\zeta} = a\zeta$). However, the leading-order eigenvalue relationship will include a because $\overline{\zeta}_1 = a/\overline{p}$ in the boundary conditions (2.27). The higher-order eigenvalue relationships will involve a because of the boundary conditions (2.29) and because of the non-homogeneous term in (2.28). Putting $\lambda \leqslant 1/4\vartheta$, we have $\eta^2 \geqslant 0$. Then the general solution of the leading-order equation (2.26) is

$$P^{(0)}(\zeta) = C_1 I_\eta(a\zeta) + C_2 K_\eta(a\zeta),$$

where I_η and K_η are the modified Bessel functions, which are known to be monotonic for any real $\eta \geqslant 0$ (Watson 1952). The boundary conditions (2.27) force us to choose $C_1 = C_2 = 0$, which leads to $P^{(0)} \equiv 0$. From equation (2.28) and boundary conditions (2.29) we get $P^{(1)} \equiv 0$. For all terms of the expansion (2.25) we will get the same result. Thus, $P \equiv 0$ and $\lambda \leqslant 1/4\vartheta$ is not an eigenvalue. A similar result is obtained with the other choices of thermal boundary conditions.

Let $\lambda > 1/4\vartheta$, then $\eta^2 < 0$. Introduce $\overline{\eta} = (\lambda\vartheta - 1/4)^{1/2}$. The modified Bessel functions $I_{i\overline{\eta}}$ and $K_{i\overline{\eta}}$ (or $I_{-i\overline{\eta}}$) are two linearly independent solutions of the leading-order equation (2.26). The real solution of (2.26) or the leading-order term of expansion (2.25) can be constructed from the real and imaginary parts of $I_{i\overline{\eta}}$ and $K_{i\overline{\eta}}$ (or $I_{-i\overline{\eta}}$):

$$P_n = C_1 \Phi(a\zeta) + C_2 \Psi(a\zeta), \tag{2.30}$$

where

$$\Phi(a\zeta) = \sum_{k=0}^{\infty} \frac{(a\zeta/2)^{2k}}{k!\, m_k} \cos(\overline{\eta}\log(\tfrac{1}{2}a\zeta) - \gamma_k), \tag{2.31}$$

$$\Psi(a\zeta) = \sum_{k=0}^{\infty} \frac{(a\zeta/2)^{2k}}{k!\, m_k} \sin(\overline{\eta}\log(\tfrac{1}{2}a\zeta) - \gamma_k). \tag{2.32}$$

Here m_k and γ_k denote the modulus and argument of the gamma function $\Gamma(k+1+\mathrm{i}\overline{\eta})$ respectively. Note that functions Φ and Ψ are analytic (see Appendix B).

$\tilde{\mathscr{Q}}$	λ_1	λ_2
0.01	661	2473
0.05	135	503
0.10	69	257
0.50	16	60
1.00	10	36

TABLE 1. The first two eigenvalues λ_1 and λ_2 for different $\tilde{\mathscr{Q}}$.

When the conducting–conducting boundary condition is imposed, constants C_1 and C_2 are both non-zero if and only if the cross-product

$$\Phi(a\zeta_1)\Psi(a\zeta_2) - \Phi(a\zeta_2)\Psi(a\zeta_1) \tag{2.33}$$

equals zero. This yields the following eigenvalue relationship:

$$\tan(\bar{\eta}\log(\zeta_2/\zeta_1)) = \frac{f(a\zeta_1)g(a\zeta_2) - f(a\zeta_2)g(a\zeta_1)}{f(a\zeta_1)f(a\zeta_2) + g(a\zeta_1)g(a\zeta_2)}. \tag{2.34}$$

Here $f(a\zeta)$ and $g(a\zeta)$ are the real and imaginary parts of the complex-valued function

$$\sum_{k=0}^{\infty} \frac{(a\zeta/2)^{2k}}{k!\Gamma(k+1+\mathrm{i}\bar{\eta})}$$

respectively.

There is an infinite number of positive roots $r_1 < r_2 < \ldots < r_n < \ldots$ of the transcendental equation (2.34) (see the graphical solutions in Appendix B), which yield the increasing sequence of positive eigenvalues

$$\lambda_n = \frac{1}{\vartheta}\left[\frac{\bar{r}_n^2 n^2\pi^2}{\log^2(1+\bar{p})} + \frac{1}{4}\right], \tag{2.35}$$

where

$$\bar{r}_n = \frac{r_n \log(1+\bar{p})}{n\pi}.$$

Since the right-hand side of (2.34) goes asymptotically to zero when $\bar{\eta}$ increases (see Appendix B), we can take $r_n\log(\zeta_2/\zeta_1) = n\pi$ and $\bar{r}_n \sim 1$ for large n. Then (2.35) becomes

$$\lambda_n \sim \frac{1}{\vartheta}\left[\frac{n^2\pi^2}{\log^2(1+\bar{p})} + \frac{1}{4}\right] \quad \text{as} \quad n \to \infty. \tag{2.36}$$

As can be seen from (2.35) and (2.36), λ_n decreases when $\tilde{\mathscr{Q}}$ increases.

The first two eigenvalues λ_1 and λ_2 calculated for $\tilde{m} = 0.02$, liquid-static pressure jump $\bar{p}_{ls} = 2.4$, $\phi = 0.03$, $a = 1$ and for different values of $\tilde{\mathscr{Q}}$ are given in table 1. The corresponding eigenfunctions for the first two modes at $\tilde{\mathscr{Q}} = 0.05$ are shown in figure 3.

The eigenfunctions P_n given by (2.19) (or (2.21)) and (2.30) generate a complete set of normal modes p_n of the form

$$p_n(x,y,\zeta,t) = \frac{P_n(\zeta)}{\zeta^{1/2}}\,\mathrm{e}^{-\lambda_n t}\,\mathrm{e}^{\mathrm{i}(\chi x+\xi y)} \quad (\xi^2+\varsigma^2 = a^2). \tag{2.37}$$

Since all eigenvalues (2.20) (or (2.22)) and (2.35) are positive, each normal mode (2.37) is stable. Hence, the pressure field is asymptotically stable.

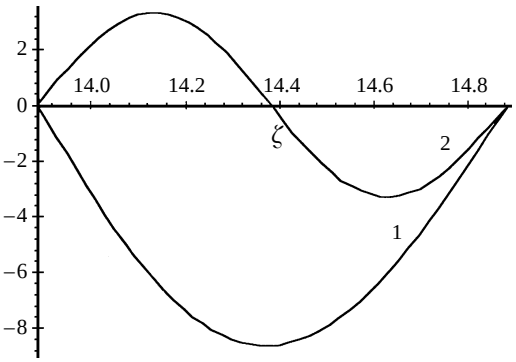

FIGURE 3. The eigenfunctions P_1 and P_2 for the first two modes; $\tilde{\mathscr{Q}} = 0.05$

The above results admit a straightforward extension to include the other choices of thermal boundary conditions. For the conducting–insulating boundary condition all eigenvalues are also positive and $\lambda = 0$ is not an eigenvalue. Thus, this case is stable. For the insulating–insulating boundary condition the complete spectrum of eigenvalues includes $\lambda = 0$ and all other eigenvalues are positive. Hence, this case is neutrally stable. The proof is identical to that given above. The eigenvalues can be computed from the zeros of cross-products of the type (2.33) with functions Φ and Ψ replaced by their derivatives at the point corresponding to the insulating boundary.

2.2. *Saturation equation*

If the pressure disturbance is known, then the saturation disturbance can be found from equation (2.10). Eliminating the Laplacian, we obtain the following linear first-order partial differential equation for k':

$$\frac{\partial k'}{\partial t} + C\,\frac{\partial k'}{\partial \zeta} = \left[\alpha_1 \frac{(\overline{p}\zeta)^{\epsilon}}{\zeta^2} + \alpha_2 \frac{(\overline{p}\zeta)^{\epsilon}}{\zeta}\right] \frac{\partial p'}{\partial t} - \alpha_3 \frac{1}{\zeta}\,\frac{\partial p'}{\partial \zeta}, \tag{2.38}$$

where

$$\alpha_1 = \frac{\dot{\psi}\overline{p}k_{rl}^{\circ}\vartheta}{\overline{p}_{ls}\tilde{m}\tilde{\mathscr{Q}}}, \quad \alpha_2 = \dot{\psi}v, \quad \alpha_3 = \frac{2\dot{\psi}\overline{p}k_{rl}^{\circ}}{\overline{p}_{ls}\tilde{m}\tilde{\mathscr{Q}}}, \quad \dot{\psi} = \left(\frac{dk_{rl}}{dS_l}\right)^{\circ}, \quad C = \dot{\psi}\,\frac{1-q}{\tilde{m}\tilde{\mathscr{Q}}}. \tag{2.39}$$

Since equation (2.38) is linear and since p' is resolved into normal modes p_n of the form (2.37), we can decompose k' into corresponding modes $k_n = K_n(\zeta, t)\,\mathrm{e}^{\mathrm{i}(\chi x + \xi y)}$ and solve equation (2.38) separately for each k_n (k_n are linearly independent due to p_n being linearly independent). To do so, we change independent variables by setting $\mathrm{d}\zeta/\mathrm{d}t = C$. This gives the family of characteristics, all of which are straight lines of slope $1/C$ since C is constant, i.e. $\zeta = Ct + r$ ($\zeta_1 \leqslant r \leqslant \zeta_2$, $\zeta_1 = 1/\overline{p}$, $\zeta_2 = 1/\overline{p} + 1$).

Equation (2.38) can be immediately integrated along characteristics and the solution is

$$K_n(r,t) = \frac{\alpha_3}{C}\left[\frac{\mathscr{P}_n(r)}{r} - \frac{\mathscr{P}_n(r+Ct)}{r+Ct}\right] - \left(\alpha_2 + \frac{\alpha_3}{C}\right)\frac{\lambda_n}{C}\mathrm{e}^{(\lambda_n/C)r} I_1(r,t) - \left(\alpha_1 + \frac{\alpha_3}{\lambda_n}\right)\frac{\lambda_n}{C}\mathrm{e}^{(\lambda_n/C)r} I_2(r,t) + K_n(r,0), \tag{2.40}$$

where $K_n(r,0)$ is the initial disturbance of the saturation field at point $r \in [\zeta_1, \zeta_2]$ and

$$I_1(r,t) = \int_r^{r+Ct} \mathscr{P}_n(s)\frac{e^{-(\lambda_n/C)s}}{s}ds, \quad I_2(r,t) = \int_r^{r+Ct} \mathscr{P}_n(s)\frac{e^{-(\lambda_n/C)s}}{s^2}ds. \tag{2.41}$$

In (2.40)–(2.41) expansion (2.23) is used.

Each solution (2.40) must satisfy hydrodynamic boundary conditions written in linearized form. If both boundaries are impermeable, then $K_n(r,t) = 0$ at $\zeta = \zeta_1, \zeta_2$ for any t. We can satisfy one boundary condition, namely that at ζ_1, by setting $K_n(\zeta_1, 0) = 0$. However, it is not possible to satisfy both boundary conditions for any $t > 0$. The standard way out of this problem is to introduce a saturation shock at ζ_2, which will be shown to be infinitesimal.

Each solution $K_n(r,t)$ of the form (2.40) can be seen as a travelling wave, which originates at some horizontal level r and moves downward with speed C. No breakdown of the solutions (2.40) is possible, since all waves $K_n(r,t)$ move at the same speed in the same direction. The development of the disturbance k' in time is fully represented by travelling waves $K_n(r,t)$. If we set the initial pressure disturbance to be zero, then, according to (2.40), the initial small disturbance of the saturation field $k'(r,0)$, represented by $K_n(r,0)$, will be transmitted along characteristics with speed C without any change in shape and size. If the porous medium is bounded in depth and $C \neq 0$, then the initial disturbance will reach the lower boundary in time $(\zeta_2 - r)/C$. A non-zero small disturbance of the pressure field excites amplified unidirectional waves in the saturation field. Again, in a bounded porous medium the 'lifetime' of these amplified disturbances does not exceed $1/C$, because the wave originated at the furthermost point ζ_1 reaches the lower boundary in this time. $1/C$ is also the time during which the growth in amplitude of the saturation waves occurs. It is important to know how much this growth is. In what follows, we show that the total amplification of the saturation waves is bounded by a multiple of the absolute maximum value of the initial pressure disturbance.

The nth component of the total amplification of the saturation wave $k'(r,t)$, originated at some point $r \in [\zeta_1, \zeta_2]$, over a distance $\zeta_2 - r$ is given by

$$\mathscr{A}_n(r) = K_n(r, (\zeta_2 - r)/C) - K_n(r,0).$$

Using the Mean Value Theorem for evaluating the integrals I_1 and I_2, we have

$$\mathscr{A}_n(r) = \frac{\alpha_3}{C}\left[\frac{\mathscr{P}_n(r)}{r} - \frac{\mathscr{P}_n(\zeta_2)e^{-(\lambda_n/C)(\zeta_2 - r)}}{\zeta_2}\right] - \mathscr{P}_n(\zeta^\sharp)\,\mathscr{N}_1 - \mathscr{P}_n(\zeta^\flat)\,\mathscr{N}_2, \tag{2.42}$$

where

$$\mathscr{N}_1(\lambda_n) = \left(\alpha_2 + \frac{\alpha_3}{C}\right)\frac{\lambda_n}{C}\,e^{(\lambda_n/C)r}\left[E_1\left(\frac{\lambda_n}{C}r\right) - E_1\left(\frac{\lambda_n}{C}\zeta_2\right)\right], \tag{2.43}$$

$$\mathscr{N}_2(\lambda_n) = \frac{\lambda_n}{C}\left(\alpha_1 + \frac{\alpha_3}{\lambda_n}\right)\left\{\frac{1}{r} - \frac{e^{-(\lambda_n/C)(\zeta_2 - r)}}{\zeta_2} - \frac{\lambda_n}{C}e^{(\lambda_n/C)r}\left[E_1\left(\frac{\lambda_n}{C}r\right) - E_1\left(\frac{\lambda_n}{C}\zeta_2\right)\right]\right\} \tag{2.44}$$

and $\zeta^\sharp, \zeta^\flat \in (r, \zeta_2)$.

In (2.43) and (2.44) E_1 is the exponential integral, i.e.

$$E_1(\zeta) = \int_\zeta^\infty \frac{e^{-s}}{s}ds.$$

Note that sequences $\{\mathscr{N}_1(\lambda_n)\}$ and $\{\mathscr{N}_2(\lambda_n)\}$ are bounded above for every fixed r.

Indeed, for $\lambda = 0$ we have

$$\lim_{\lambda \to 0} \left[\frac{\lambda}{C} E_1 \left(\frac{\lambda}{C} \zeta \right) \right] = 0$$

and, hence,

$$\mathscr{N}_1(0) = 0, \quad \mathscr{N}_2(0) = \frac{\alpha_3}{C} \left(\frac{1}{r} - \frac{1}{\zeta_2} \right) < \infty.$$

For $\lambda_n \to \infty$ (high eigenvalues) we have

$$\mathscr{N}_1(\lambda_n) \sim \left(\alpha_2 + \frac{\alpha_3}{C} \right) \frac{1}{r} + O\left(\frac{1}{\lambda_n} \right), \quad \mathscr{N}_2(\lambda_n) \sim \alpha_1 \frac{1}{r^2} + O\left(\frac{1}{\lambda_n} \right). \tag{2.45}$$

In expressions (2.45) the following asymptotic expansion for the exponential integral is used (Abramowitz & Stegun 1968):

$$\frac{\lambda}{C} E_1 \left(\frac{\lambda}{C} \zeta \right) \sim \frac{\mathrm{e}^{-(\lambda/C)\zeta}}{\zeta} \left\{ 1 - \frac{C}{\lambda \zeta} + 1 \times 2 \left(\frac{C}{\lambda \zeta} \right)^2 - 1 \times 2 \times 3 \left(\frac{C}{\lambda \zeta} \right)^3 + \ldots \right\}.$$

Therefore for every fixed $r \in [\zeta_1, \zeta_2]$ there exist finite numbers $\mathscr{N}_1^*$ and $\mathscr{N}_2^*$, not depending on n, such that $\mathscr{N}_{1,2}(\lambda_n) \leqslant \mathscr{N}_{1,2}^*$ for all λ_n. Recalling that the total amplification $\mathscr{A}(r) = \sum_{n=1}^{\infty} c_n \mathscr{A}_n(r) \mathrm{e}^{\mathrm{i}(\chi x + \xi y)}$, where c_n are the coefficients in the normal mode expansion of p', we can write

$$|\mathscr{A}(r)| \leqslant \mathscr{P}^* \mathscr{N}_r, \tag{2.46}$$

where

$$\mathscr{N}_r = \frac{\alpha_3}{C} \frac{1}{r} + \mathscr{N}_1^* + \mathscr{N}_2^*$$

and

$$\mathscr{P}^* = \max_{\zeta \in [\zeta_1, \zeta_2]} \{ |p'(\zeta, 0)| \}.$$

According to (2.46), the total amplification of the saturation wave k' does not exceed the absolute maximum value of the initial pressure disturbance multiplied by the finite number $\mathscr{N}_r$. This also means that it is possible to make the total amplification of k' to be as small as we wish. In other words, k' remains small for all times provided the initial pressure disturbance is small. Thus, the saturation field is stable. (Here we talk about stability in the sense of Lyapunov as defined in Drazin & Reid 1981.)

Setting $r = \zeta_1$ and assuming the conducting–conducting boundary condition at $\zeta = \zeta_1$ and $\zeta = \zeta_2$, we have

$$\mathscr{N}_{\zeta_1} = \left(\alpha_2 + \frac{\alpha_3}{C} \right) \bar{p} + \alpha_1 \bar{p}. \tag{2.47}$$

As follows from (2.47), $\mathscr{N}_{\zeta_1}$ is small, since $\bar{p}$ is small in a vapour-dominated flow. Note that the absolute value of the total amplification of the saturation wave originated at the upper boundary, $|\mathscr{A}(\zeta_1)|$, gives the magnitude of the saturation shock at ζ_2, which is infinitesimal according to (2.46). The bounding number $\mathscr{N}_{\zeta_1}$ and wave speed C, calculated for linear relative permeabilities ($\psi = 1$) and for Grant's curves ($\psi \neq 1$) (Grant, Donaldson & Bixley 1982), are given in table 2. Here we take $\tilde{m} = 0.02$, $\bar{p}_{ls} = 2.4$, $\phi = 0.03$, residual saturations $S_{rl} = 0.25$ and $S_{rv} = 0.05$. Values of C and $\mathscr{N}_{\zeta_1}$ are calculated using the exact steady-state solutions. According

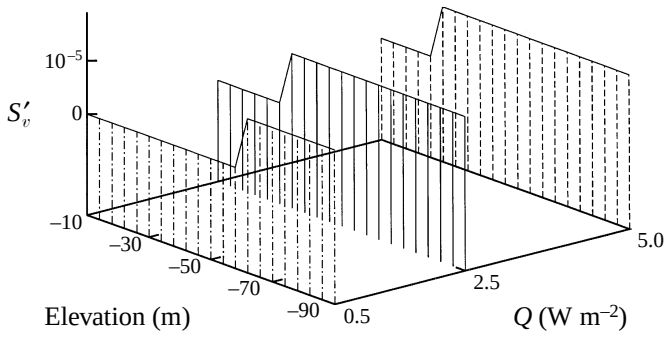

FIGURE 4. The saturation disturbance after 0.501×10^8 s.

$\tilde{\mathscr{Q}}$	C ($\dot{\psi}=1$)	$\mathscr{N}_{\zeta_1}$ ($\dot{\psi}=1$)	C ($\dot{\psi}\neq 1$)	$\mathscr{N}_{\zeta_1}$ ($\dot{\psi}\neq 1$)
0.01	4890	0.2	47.7	0.0019
0.05	970	0.3	31.6	0.0085
0.10	480	0.4	26.3	0.0193
0.50	88	1.1	16.1	0.2100
1.00	38	2.4	12.4	0.7299
1.50	22	4.3	11.9	2.4000
2.00	13	7.1	11.0	5.7010
2.50	8	12.6	9.7	14.7558

TABLE 2. C and $\mathscr{N}_{\zeta_1}$ for different $\tilde{\mathscr{Q}}$.

to our calculations, C is large compared to 1 for $\tilde{\mathscr{Q}} \ll \tilde{\mathscr{Q}}^{cr}$, and it is decreasing when $\tilde{\mathscr{Q}}$ is increasing. This can be seen from the analytical expression (2.39) too. The bounding number $\mathscr{N}_{\zeta_1}$ is increasing when $\tilde{\mathscr{Q}}$ is increasing, and it is relatively large for $\tilde{\mathscr{Q}} \sim \tilde{\mathscr{Q}}^{cr}$.

Let us define the relaxation time τ as equal to $1/|C|$. Then, for the states with $\tilde{\mathscr{Q}} \lesssim 1$, relaxation time τ is small compared to 1. (Returning to dimensional quantities, the relaxation time is much less than the characteristic time t^*.) Time τ is increasing when $\tilde{\mathscr{Q}}$ is increasing (see table 2). According to our calculations, the states with $\tilde{\mathscr{Q}} \sim \tilde{\mathscr{Q}}^{cr}$ (sub-critical states) equilibrate to the initial unperturbed state relatively slowly, and the saturation field remains perturbed during relatively long periods of time. Moreover, the saturation disturbance may grow one order of magnitude larger than the initial pressure disturbance since $\mathscr{N}_{\zeta_1} \sim 10$ for sub-critical states (see table 2).

To verify the above analytical results we performed computer simulations using the numerical program TOUGH2 (Pruess 1986). The initial unperturbed state was set to be one-dimensional vapour-dominated counterflow. A constant temperature and constant heat flux were imposed at the upper and lower boundary respectively. In all simulations, the upper layers of the vapour-dominated region equilibrated first. As expected, the saturation field exhibited high sensitivity to small disturbances of pressure. There was a strong indication that the wave speed of the saturation disturbances decreases when $\tilde{\mathscr{Q}}$ increases. To illustrate this, figure 4 shows the saturation disturbance S'_v after 0.501×10^8 s for three values of Q. The reservoir permeability was taken to be 10^{-14} m^2. Other parameters used in figure 4 were chosen to be

representative of the Geysers geothermal field (Lai *et al.* 1994). Pressure was slightly perturbed at $t = 0$ near the top of the reservoir (-18 m in figure 4).

3. Conclusions

The purpose of this theoretical investigation was to explain the development of two-layer structures within homogeneous geothermal reservoirs. The presence of two superposed layers, saturated by water and steam in different proportions, was inferred from measurements in the Wairakei, Geysers and Larderello geothermal fields. There was no drilling evidence of any permeability contrasts and low permeability barriers between the two layers. As we conjectured earlier (Pestov 1995), these two-layer structures may result from time changes in the vertical heat flow, reservoir permeability, and the total mass of water in the system.

In this paper we introduce the quasi-static approximation for geothermal processes and examine the stability of vapour-dominated counterflow looking at the development in time of both pressure and saturation disturbances. For the vapour-dominated case the system of linearized governing equations can be decoupled and a separate parabolic equation for the pressure disturbance can be obtained. After determining the pressure disturbance, the saturation disturbance can be found from the remaining travelling wave equation.

We treat the pressure and saturation equations by the method of normal modes and the method of characteristics respectively. The pressure field is shown to be asymptotically stable for all choices of thermal boundary conditions excluding the insulating–insulating boundary condition for which it is neutrally stable. According to our results, the pressure field is not sensitive to small disturbances of the saturation field, whereas the saturation field is highly sensitive to small disturbances of pressure. Small disturbances of pressure excite unidirectional amplified waves in the saturation field which propagate with the same constant speed. When the initial pressure disturbance is set to be zero, an initial small disturbance of the saturation field is transmitted towards the lower boundary without any change in shape. The saturation field is proven to be stable in the sense of Lyapunov, that is, the saturation disturbance remains bounded by an infinitesimal number for all times.

We define the relaxation time to restore equilibrium as $\tau = 1/|C|$, where C is the wave speed of the saturation disturbances. The absolute value of C determines the 'lifetime' of the amplified saturation waves: in time $1/|C|$ all saturation waves leave the flow region. The sign of C determines the direction of propagation of the saturation waves. In vapour-dominated counterflow, the wave speed is positive and hence the saturation waves propagate towards the lower boundary. In liquid-dominated counterflow, the wave speed is negative and the saturation waves propagate upward to the upper boundary. The signs of the wave speed derived from the linearized saturation equations are the same as those deduced from numerical experimenting with nonlinear equations by Kissling *et al.* (1992). The direction of propagation of small saturation waves specifies the location of a two-phase zone within a system and explains why the inverse structures IA, IB, IC, and ID are not realized in nature.

In the case of vapour-dominated counterflow, the relaxation time calculated from the linearized saturation equation is short compared to the characteristic time when $\tilde{\mathcal{Q}} \lesssim 1$. The relaxation time increases when $\tilde{\mathcal{Q}}$ increases. For $\tilde{\mathcal{Q}} \sim \tilde{\mathcal{Q}}^{cr}$ (sub-critical states) the saturation field remains perturbed during longer periods of time and the saturation disturbances may grow one order of magnitude larger than the initial

pressure disturbance. This may indicate that the sub-critical states are becoming transient (Zemansky 1957; Callen 1985).

Given the direction of propagation of saturation disturbances, we conclude that the upper layers of a vapour-dominated zone equilibrate earlier than its lower layers. Hence, the vapour-dominated zone always adhers to the upper boundary of a porous medium provided it was there at previous times.

Let us assume that at $t = 0$ a porous medium is fully two-phase and vapour-dominated, and $\tilde{\mathcal{Q}}$ is much less than 1. According to our results, the relaxation time is short compared to the characteristic time until $\tilde{\mathcal{Q}} \lesssim 1$. Then the two-layer structures of types A, B and C can be connected to this initial state by a quasi-static path. Since the initial state is a steady state, structures A, B and C are also steady states (Zemansky 1957; Callen 1985). We may conclude that structures A, B and C can develop during the evolution of a vapour-dominated geothermal system. On the other hand, there is no quasi-static path between any vapour-dominated steady state (e.g. a fully two-phase vapour-dominated steady state and steady states of types A, B and C) and the inverse two-layer structures I A, I B and I C. Therefore inverse structures I A, I B and I C cannot develop during the evolution of a vapour-dominated geothermal system.

It is also unlikely that structures I A, I B and I C can develop from a fully two-phase liquid-dominated initial state. Let us assume that the initial state of a system is fully two-phase and liquid-dominated, the final state is either I C or I A, and the transition is quasi-static. According to the results of Appendix C, it is theoretically possible that a structure with a water layer over a liquid-dominated counterflowing zone, model D, develops from a fully two-phase liquid-dominated steady state when $\tilde{\mathcal{Q}}$ increases. (Given the direction of propagation of saturation disturbances, the inverse structure ID is impossible – see Appendix C.) Then a further increase in $\tilde{\mathcal{Q}}$ would lead to the formation of I C or I A if the system could pass through the critical point $\tilde{\mathcal{Q}}^{cr}$ (see figure 1). Such a quasi-static transition, however, is impossible. There is an indication coming from our analytical results presented here and supported by our earlier numerical investigations (Pestov 1995), that the sub-critical states are not steady. This also agrees with the numerical investigations of nonlinear equations by Weir & Young (1991). According to their results, it is not possible for a liquid-dominated zone to switch to vapour-dominated conditions by passing the critical point for the heat flux value, since the wave speed becomes zero there and hence the relaxation time grows infinitely large.

We may conclude that there are no quasi-static paths between the fully two-phase liquid-dominated state and the inverse two-layer structures I A, I B and I C. We also may conclude that I A, I B and I C cannot develop from a fully two-phase liquid-dominated initial state either. The latter explains why structures similar to I A, I B and I C have never been found in nature.

It is, however, possible to transform steady states A, C and a fully two-phase vapour-dominated steady state into a fully two-phase liquid-dominated state by changing the total amount of water and holding the dimensionless heat flux fixed. Using the model of the quasi-permeable boundary introduced in Pestov (1996), one can construct a quasi-static path to a fully two-phase liquid-dominated steady state. (It is possible to find values of $\tilde{\mathcal{Q}}$ for which liquid-dominated counterflow is stable, as shown numerically in Pestov 1995.) Such a quasi-static path will represent some injection/withdrawal process.

Structures A, B and C were obtained numerically from a fully two-phase vapour-dominated steady state in Pestov (1995).

The present results do not apply to regions with lateral flows and large mass recharges.

This research was supported by a Victoria University of Wellington Postgraduate Scholarship for PhD study, which is gratefully acknowledged. I thank my supervisors Mark McGuinness and Graham Weir for continued help. I am indebted to Phil Broadbridge, Robert McKibbin, Don Nield, Boris Pavlov, Vladimir Pestov, and to the referees of this paper for useful comments.

Appendix A. Quasi-static process

A quasi-static process is a series of simultaneous transitions from one equilibrium state to the neighbouring equilibrium state caused by an infinitesimal unbalanced force. During each transition parameters of the system change by an infinitesimal amount. However, changes over sufficiently long periods of time may be finite.

Suppose that some parameter of the system k changes over a period of time $t_n - t_0$, which is long compared to the characteristic time of the system t^*, i.e. $t_n - t_0 \gg t^*$. We say that process $k(t)$ is *slow* if the variation of k over any time interval $I \subseteq [t_0, t_n]$ of length t^* is small compared to the minimum value of k on the same interval I:

$$\omega(k, I) = \max_{t \in I} k(t) - \min_{t \in I} k(t) \ll \min_{t \in I} k(t).$$

Note that the variation of k over the whole interval $[t_0, t_n]$, $\omega(k, [t_0, t_n])$, can be large. In a particular case where process $k(t)$ is smooth ($k(t)$ is a differentiable function), this is equivalent to the following condition on the derivative $\mathrm{d}k/\mathrm{d}t$ at any t, $t_0 \leqslant t \leqslant t_n$:

$$\frac{\mathrm{d}k(t)}{\mathrm{d}t} \ll \min_{t \in I} k(t) \frac{1}{t^*},$$

where I is the interval of length t^* centred at t.

When process $k(t)$ is slow, it is possible to find a partition, $\Pi = \{t_0, t_1, \ldots, t_{n-1}, t_n\}$, of the interval $[t_0, t_n]$, such that the mesh, $\mathrm{mesh}\Pi = \min_{i=0}^{n-1}\{t_{i+1} - t_i\}$, of Π is greater than or similar to t^* and the variation of k on each interval $I_i = [t_{i+1}, t_i]$, $\omega(k, I_i) = \max_{t \in I_i} k(t) - \min_{t \in I_i} k(t)$, is much less than $\min_{t \in I_i} k(t)$, that is

$$\min_{i=0}^{n-1}\{t_{i+1} - t_i\} \gtrsim t^*, \tag{A 1}$$

$$\max_{t \in I_i} k(t) - \min_{t \in I_i} k(t) \ll \min_{t \in I_i} k(t). \tag{A 2}$$

Now the original slow process $k(t)$ is approximated by a quasi-static path, every i-step of which can be described in the following manner. Assume that at $t < t_i$ the system is at the state of thermodynamic equilibrium. At time $t = t_i$, called here *the event time*, we change parameter k instantly by a small amount and wait until the system equilibrates to a new equilibrium state. The time, τ, during which an equilibrium state can be restored, is called the relaxation time of the system. If for any i ($i = 0, ..., n-1$) we have $\tau \ll t_{i+1} - t_i$, then process $k(t)$ can be replaced by a series of instantaneous transitions between neighbouring equilibrium states, and for any $t \in I_i$, $i = 0, ..., n-1$ the steady-state conditions can be applied. In other words, the final state of the system, $\mathscr{S}(t_n)$, is accessible from the initial sate, $\mathscr{S}(t_0)$, by the quasi-static path. If for some i^{cr} : $0 < i^{cr} < n$ the relaxation time τ becomes comparable with $t_{i+1} - t_i$ and if it is not possible to dissect the interval $[t_0, t_n]$ further satisfying conditions (A 1) and (A 2), then the state of the system cannot be described

in terms of spatial coordinates only and must involve time. The steady state conditions are not applicable anymore, and the system passes through non-equilibrium states. In other words, the state $\mathscr{S}(t_n)$ is not accessible from the steady-state $\mathscr{S}(t_0)$ by the quasi-static path. If there is no other quasi-static path between $\mathscr{S}(t_n)$ and $\mathscr{S}(t_0)$, then $\mathscr{S}(t_n)$ is not an equilibrium state (Zemansky 1957; Callen 1985).

Appendix B. Functions of the Φ and Ψ families

Since the modified Bessel function $I_{-i\overline{\eta}}$ is the complex conjugate of $I_{i\overline{\eta}}$, the real-valued solution of (2.26) can be constructed from the real and imaginary parts of $I_{i\overline{\eta}}$, i.e.

$$\Phi = \mathrm{Re}\left(I_{i\overline{\eta}}\right), \quad \Psi = \mathrm{Im}\left(I_{i\overline{\eta}}\right)$$

or in the form of series

$$\Phi(\zeta) = \sum_{k=0}^{\infty} \frac{(\frac{1}{2}\zeta)^{2k}}{k!m_k} \cos(\overline{\eta}\log\tfrac{1}{2}\zeta - \gamma_k),$$

$$\Psi(\zeta) = \sum_{k=0}^{\infty} \frac{(\frac{1}{2}\zeta)^{2k}}{k!m_k} \sin(\overline{\eta}\log\tfrac{1}{2}\zeta - \gamma_k),$$

where m_k and γ_k are the modulus and argument of the gamma function $\Gamma(k+1+i\overline{\eta})$ respectively. (Here we take $a = 1$.)

We shall show that functions Φ and Ψ are analytic in the right half-plane $\mathrm{Re}(\zeta) > 0$, and, as a corollary, they are real analytic functions in the positive half-axis $\zeta > 0$. Since every term of the series Φ and Ψ is an analytic function in $\mathrm{Re}(\zeta) > 0$ being a composition of analytic functions, it is sufficient to show that both series converge uniformly on every compact subset of $\mathrm{Re}(\zeta) > 0$.

Let D be a compact subset of $\mathrm{Re}(\zeta) > 0$. Without loss in generality for some real a, b, c, where $0 < a < b$ and $c > 0$, D is contained in the region determined by inequalities

$$a \leqslant \mathrm{Re}(\zeta) \leqslant b, \quad -c \leqslant \mathrm{Im}(\zeta) \leqslant c.$$

In particular, for any $\zeta \in D$, as follows from formula (4.1.2) of Abramowitz & Stegun (1968),

$$|\zeta| \leqslant (c^2 + b^2)^{1/2}, \quad |\ln\zeta/2| = |\ln|\zeta/2| + i\theta_\zeta| \leqslant |\ln((c^2+b^2)^{1/2}/2)| + \pi,$$

where θ_ζ is the argument of ζ, $-\pi < \theta_\zeta < \pi$.

Therefore, if $\zeta \in D$, then

$$\begin{aligned}
|\cos(\overline{\eta}\log\tfrac{1}{2}\zeta - \gamma_k)| &= |\cos(\overline{\eta}\log\tfrac{1}{2}\zeta)\cos\gamma_k + \sin(\overline{\eta}\log\tfrac{1}{2}\zeta)\sin\gamma_k| \\
&\leqslant |\cos(\overline{\eta}\log\tfrac{1}{2}\zeta)|\,|\cos\gamma_k| + |\sin(\overline{\eta}\log\tfrac{1}{2}\zeta)|\,|\sin\gamma_k| \\
&\leqslant |\cos(\overline{\eta}\log\tfrac{1}{2}\zeta)| + |\sin(\overline{\eta}\log\tfrac{1}{2}\zeta)| \\
&\leqslant |\cos(\overline{\eta}\,\mathrm{Re}[\log\tfrac{1}{2}\zeta])|\,|\cosh(\overline{\eta}\,\mathrm{Im}[\log\tfrac{1}{2}\zeta])| \\
&\quad + |\sin(\overline{\eta}\,\mathrm{Re}[\log\tfrac{1}{2}\zeta])|\,|\sinh(\overline{\eta}\,\mathrm{Im}[\log\tfrac{1}{2}\zeta])| \\
&\quad + |\sin(\overline{\eta}\,\mathrm{Re}[\log\tfrac{1}{2}\zeta])|\,|\cosh(\overline{\eta}\mathrm{Im}[\log\tfrac{1}{2}\zeta])| \\
&\quad + |\cos(\overline{\eta}\,\mathrm{Re}[\log\tfrac{1}{2}\zeta])|\,|\sinh(\overline{\eta}\,\mathrm{Im}[\log\tfrac{1}{2}\zeta])| \\
&\leqslant 2\exp(\overline{\eta}\,\mathrm{Im}[\log\tfrac{1}{2}\zeta]) \leqslant 2\exp(\overline{\eta}|\log\tfrac{1}{2}\zeta|) \\
&\leqslant 2e^{\overline{\eta}}\exp[|\log\tfrac{1}{2}(c^2+b^2)^{1/2}| + \pi].
\end{aligned}$$

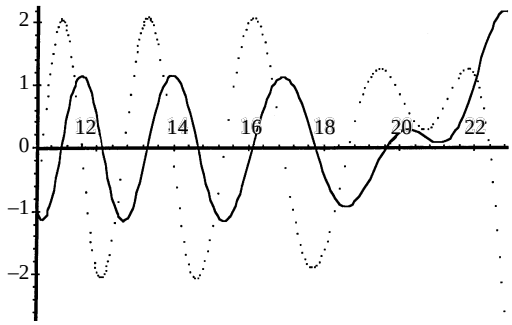

FIGURE 5. The functions of the Φ and Ψ families at $\tilde{\mathscr{Q}} = 0.1$.

Here formulas (4.3.17), (4.3.55) and (4.3.56) of Abramowitz & Stegun (1968) are used.

As a corollary, for every $k \geqslant 1$ and $\zeta \in D$ we have

$$\left| \frac{(\frac{1}{2}\zeta)^{2k}}{k!m_k} \cos(\overline{\eta} \log \tfrac{1}{2}\zeta - \gamma_k) \right| \leqslant \frac{(b^2 + c^2)^k}{4^k k! m_k} 2\,\mathrm{e}^{\overline{\eta}} \exp[|\log \tfrac{1}{2}(c^2 + b^2)^{1/2}| + \pi],$$

and since $m_k \to \infty$ as $k \to \infty$, we further have

$$\left| \frac{(\zeta/2)^{2k}}{k!m_k} \cos(\overline{\eta} \log \tfrac{1}{2}\zeta - \gamma_k) \right| \leqslant \frac{C_1^k}{k!} C_2,$$

where C_1, C_2 are positive constants. Note that series $\sum C_1^k/k!$ is convergent. Hence, Φ is uniformly convergent in the region D. Therefore we conclude from Weierstrass's theorem that Φ is analytic. A similar argument works for Ψ.

Functions Φ and Ψ behave as periodic functions in the interval $[\zeta_1, \zeta_1 + 1]$ for $\zeta_1 = 1/\overline{p}$, representative of geothermal reservoirs. This means that it is possible to satisfy the thermal boundary conditions for the pressure disturbance at both ends by stretching these functions in an appropriate way.

However, when $\zeta \to \infty$ functions Φ and Ψ are amplified exponentially. Indeed, for all natural k we have (formula (6.1.16) of Abramowitz & Stegun 1968)

$$m_k \geqslant k!\,|\Gamma(1 + \mathrm{i}\overline{\eta})| = k!\,m_\circ.$$

Therefore, if ζ is real positive,

$$|\Phi(\zeta)| \leqslant \sum_{k=0}^{\infty} \left| \frac{\frac{1}{2}\zeta^{2k}}{k!m_k} \cos(\overline{\eta} \ln \tfrac{1}{2}\zeta - \gamma_k) \right| \leqslant \frac{1}{m_\circ} \sum_{k=0}^{\infty} \frac{\zeta^{2k}}{2^{2k}(k!)^2}$$
$$\leqslant \frac{1}{m_\circ} \sum_{k=0}^{\infty} \frac{\zeta^{2k}}{(2 \times 4 \times \cdots \times 2k)^2} \leqslant \frac{1}{m_\circ} \sum_{k=0}^{\infty} \frac{\zeta^{2k}}{(2k)!} \leqslant \frac{\cosh \zeta}{m_\circ}.$$

Thus for large ζ

$$\Phi \lesssim \frac{1}{|\Gamma(1 + \mathrm{i}\overline{\eta})|} \cosh(\zeta), \text{ and similarly, } \Psi \lesssim \frac{1}{|\Gamma(1 + \mathrm{i}\overline{\eta})|} \cosh(\zeta).$$

Figure 5 shows the functions of the Φ and Ψ families for the first mode at $\tilde{\mathscr{Q}} = 0.1$. Function Φ is represented by a line and function Ψ is represented by points; both are normalized by their values at ζ_2. In figure 5 we take $\tilde{m} = 0.02$, $\overline{p}_{ls} = 2.4$ and $\phi = 0.03$

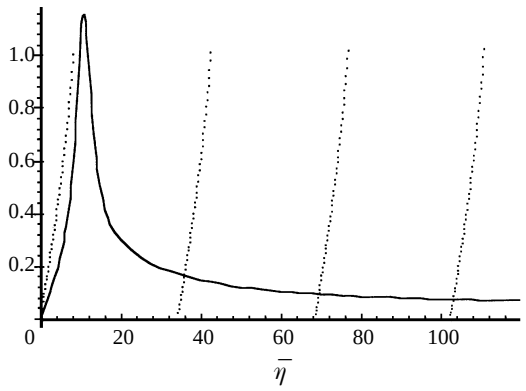

FIGURE 6. A graphical solution of equation (2.34) at $\tilde{\mathcal{Q}} = 0.1$.

After writing the cross-product of Φ and Ψ in the form (2.34), its zeros can be easily calculated, e.g. with the help of the Maple system. The graphical solution for $\tilde{\mathcal{Q}} = 0.1$ is presented in figure 6 ($a = 1$ in both cases). The left-hand side of (2.34) is represented by points, and the right-hand side of (2.34) is represented by a line. The plotted solution demonstrates that the right-hand side goes asymptotically to zero when $\bar{\eta}$ increases, and that there is an infinite number of positive zeros of the cross-product (2.33).

Appendix C. On the stability of liquid-dominated counterflow

For the liquid-dominated basic state it is not possible to obtain a separate equation for the pressure disturbance. In regard to the stability question, we rely on numerous computer experiments that simulated a stable liquid-dominated counterflow in a range of parameters typical of two-phase reservoirs (see, for example, Lai *et al.* 1994; Pestov 1995, 1997). A stable liquid-dominated counterflow was also obtained in laboratory experiments by Bau & Torrance (1982).

Here we determine the direction of propagation of small saturation disturbances in the liquid-dominated medium. In this case the simplified equations (2.8)–(2.10) can be also used when $\tilde{\mathcal{Q}} \gg \tilde{\kappa}$. Here $\tilde{\kappa}$ is the lower bound for the existence of liquid-dominated counterflow (McGuinness & Pestov 1996). Now coefficients in (2.8)–(2.10) must be calculated from the liquid-dominated steady solution. For this solution we have (Pestov 1996)

$$k_{rv}^{\circ} = \frac{\mu\tilde{\mathcal{Q}}}{\varphi^{\circ}(1-\tilde{m}\varphi^{\circ})} \sim \mu\tilde{\mathcal{Q}} \ll k_{rl}^{\circ} \sim 1 \Rightarrow \psi \sim 1,\ k_{rl}^{\circ} \sim k_{rv}^{\circ}/\mu\tilde{\mathcal{Q}};$$

$$q = 1 - \tilde{m}\tilde{\mathcal{Q}} \Rightarrow c_v \sim 1/\mu\tilde{\mathcal{Q}} \gg c_l = 1.$$

Note that k_{rl}°, ψ, q, c_l and c_v vary with z only slightly and φ° can be taken as a linear function of z when $\tilde{\mathcal{Q}}$ is small compared to $\tilde{\mathcal{Q}}^{cr}$.

For the sake of simplicity, we restrict our consideration to $\tilde{\mathcal{Q}} \gg \tilde{\kappa}$ and $\tilde{\mathcal{Q}} \ll \tilde{\mathcal{Q}}^{cr}$. In practice it is possible to satisfy both of these inequalities. For instance, if $k = 10^{-13}$ m^2, then $\tilde{\kappa} \sim 10^{-3}$ and $\tilde{\mathcal{Q}}^{cr} = 2.8$ (Pestov 1996), and there is a non-zero interval of $\tilde{\mathcal{Q}} : 10^{-3} \ll \tilde{\mathcal{Q}} \ll 1$.

Eliminating the Laplacian from (2.8)–(2.10), we have

$$\frac{\tilde{m}}{\dot{\psi}}\left(1+\frac{\tilde{\mathcal{Q}}}{k^{\circ}_{rl}}\frac{k^{\circ}_{rv}}{\mu\tilde{\mathcal{Q}}}\right)\varphi^{\circ}\frac{\partial k'_{rv}}{\partial t}-c_v\Bigg(1-\underbrace{\frac{c_l}{c_v}\frac{\tilde{m}\tilde{\mathcal{Q}}}{k^{\circ}_{rl}}\frac{k^{\circ}_{rv}}{\mu\tilde{\mathcal{Q}}}}_{O(\tilde{m}\mu\tilde{\mathcal{Q}}^2)}\Bigg)\varphi^{\circ}\frac{\partial k'_{rv}}{\partial z}-c_v\frac{\mathrm{d}\varphi^{\circ}}{\mathrm{d}z}k'_{rv}=\Phi_1[p'],$$

where

$$\Phi_1[p']=\frac{\overline{p}}{\overline{p}_{ls}}\left(\frac{\Phi_v}{\mu\tilde{\mathcal{Q}}}-\frac{1}{k^{\circ}_{rl}}\frac{k^{\circ}_{rv}}{\mu\tilde{\mathcal{Q}}}\varphi^{\circ}\Phi_l\right)$$

is the first-order linear differential operator. On noting that the under-braced coefficient is small compared to 1, the above equation can be rewritten in the form

$$\frac{\partial\rho'}{\partial t}+C\frac{\partial\rho'}{\partial z}=\frac{\dot{\psi}}{\tilde{m}}\frac{1}{1+k^{\circ}_{rv}/k^{\circ}_{rl}\mu}\Phi_1[p'], \tag{C 1}$$

where $\rho'=\varphi^{\circ}k'_{rv}$ and

$$C=-\frac{\dot{\psi}}{\tilde{m}}\frac{q-\tilde{m}\varphi^{\circ}}{\mu\tilde{\mathcal{Q}}+\tilde{\mathcal{Q}}k^{\circ}_{rv}/k^{\circ}_{rl}}. \tag{C 2}$$

Note that C in (C 2) is negative. Kissling *et al.* (1992) and Young (1996) also obtained a negative saturation wave speed for the liquid-dominated solution. An important corollary of this result is that small saturation disturbances propagate upward from the bottom to the top of a reservoir. Assuming that the pressure field is stable, we may conclude that the lower layers of a liquid-dominated zone equilibrate earlier than the upper layers. We may also conclude that there is a quasi-static path between the fully two-phase liquid-dominated steady state and structure D, and that structure D is a steady state. Given the direction of propagation of saturation disturbances, the inverse structure ID is impossible.

REFERENCES

Abramowitz, M. & Stegun, I. A. 1968 *Handbook of Mathematical Functions*. Dover.

Allis, R. G. & Hunt, M. 1986 Analysis of exploitation-induced gravity changes at Wairakei geothermal field. *Geophysics* **51**, 1647–1660.

Barenblatt, G. I., Entov, V. M. & Ryzhik, V. M. 1990 *Theory of Fluid Flows through Natural Rocks*. Kluwer.

Bau, H. H. & Torrance, K. E. 1982 Boiling in low-permeability porous materials. *Intl J. Heat Mass Transfer* **25**, 45–54.

Bear, J. & Bachmat, Y. 1991 *Introduction to Modeling of Transport Phenomena in Porous Media*. Kluwer.

Callen, H. B. 1985 *Thermodynamics and an Introduction to Thermostatistics*. John Wiley & Sons.

Cheng, P. 1978 Heat transfer in geothermal systems. *Adv. Heat Transfer* **14**, 1–105.

Drazin, P. G. & Reid, W. H. 1981 *Hydrodynamic Stability*. Cambridge University Press.

Drenick, A. 1986 Pressure-temperature-spinner survey in a well at The Geysers. In *Proc. 11th Workshop Geother. Reservoir Engng, Stanford University*, pp. 197–206.

Garg, S. K. & Pritchett, J. W. 1977 On pressure-work, viscous dissipation and the energy balance relation for geothermal reservoirs. *Adv. Water Res.* **1**, 41–47.

Grant, M. A., Donaldson, I. G. & Bixley, P. F. 1982 *Geothermal Reservoir Engineering*. Academic.

Kissling, W., McGuinness, M., Weir, G., White, S. & Young, R. 1992 Vertical two-phase flow in porous media. *Transp. Porous Media*, **8**, 99–131.

Lai, C. H., Bodvarsson, G. S. & Truesdell, A. H. 1994 Modeling studies of heat transfer and phase distribution in two-phase geothermal reservoirs. *Geothermics*, **23**, 3–20.

McGuinness, M. J. 1996 Steady solution selection and existence in geothermal heat pipes – I. The convective case. *Intl J. Heat Mass Transfer* **39**, 259–274.

McGuinness, M. J. 1997 Steady solution selection and existence in geothermal heat pipes – II. The conductive case. *Intl J. Heat Mass Transfer* **40**, 311–321.

McGuinness, M. J., Blakeley, M., Pruess, K. & O'Sullivan, M. J. 1993 Geothermal heat pipe stability: solution selection by upstreaming and boundary conditions. *Transp. Porous Media* **11**, 71–100.

McGuinness, M. & Pestov, I. 1996 Non-balanced counter flow; the effects of net mass flux. In *Proc. 18th New Zealand Geothermal Workshop, University of Auckland*, pp. 281–284.

O'Sullivan, M. J., Zyvoloski, G. A. & Blakeley, M. 1983 Computer modelling of geothermal reservoirs. School of Engineering Report, 318. University of Auckland, Auckland.

Pestov, I. 1994 Mathematical modelling of vapour-dominated geothermal systems. In *Proc. 16th New Zealand Geothermal Workshop, University of Auckland, Auckland*, pp. 29–32.

Pestov, I. 1995 Modelling studies of the evolution of vapour-dominated geothermal systems. In *Proc. 17th New Zealand Geothermal Workshop, University of Auckland*, pp. 199–204.

Pestov, I. 1996 Mathematical modelling of two-phase geothermal systems. PhD thesis, Victoria University of Wellington, Wellington, New Zealand.

Pestov, I. 1997 Modelling structured geothermal systems: application of dimensional methods. *Mathematical and Computer Modelling* **25**, 43–63.

Pruess, K. 1986 TOUGH user's guide. *Lawrence Berkeley Laboratory* Rep. LBL-20700.

Pruess, K., Celati, R., Calore, C. & Cappetti, G. 1987 On fluid and heat transfer in deep zones of vapor-dominated geothermal reservoirs. In *Proc. 12th Workshop Geother. Reservoir Engng, Stanford University*, pp. 89–96.

Ramesh, P. S. & Torrance, K. E. 1990 Stability of boiling in porous media. *Intl J. Heat Mass Transfer* **33**, 1895–1908.

Ramesh, P. S. & Torrance, K. E. 1993 Boiling in a porous layer heated from below: effects of natural convection and a moving liquid/two-phase interface. *J. Fluid Mech.* **257**, 289–309.

Schubert, G. & Straus, J. M. 1980 Gravitational stability of water over steam in vapor-dominated geothermal systems. *J. Geophys. Res.* **85**, 6505–6512.

Shook, M. 1993 Numerical investigations into the formation of a high temperature reservoir. In *Proc. 18th Workshop Geother. Reservoir Engng, Stanford University*, pp. 91–95.

Thomas, R. P., Chapman, R. H., Dykstra H. & Stockton, A. D. 1981 A Reservoir Assessment of The Geysers Geothermal Field. *Cal. Dept. of Conservation,* TR27.

Truesdell, A. H. 1991 The origin of high-temperature zones in vapor-dominated geothermal systems. In *Proc. 16th Workshop Geother. Reservoir Engng, Stanford University*, pp. 15–20.

Walters, M. A., Strenfeld, J. N., Haizlip, J. R., Drenick, A. F. & Combs J. 1988 A vapor-dominated reservoir exceeding 600°*F* at The Geysers, Sonoma County, California. In *Proc. 13th Workshop Geother. Reservoir Engng, Stanford University*, pp. 73–81.

Watson, G. N. 1952 *A Treatise on the Theory of Bessel Functions*. Cambridge University Press.

Weir, G. J. & Young, R. M. 1991 Quasi-steady vertical two-phase flows in porous media. *Water Resour. Res.* **27**, 1207–1214.

White, D. E., Muffler, L. J. P. & Truesdell, A. H. 1971 Vapor-dominated hydrothermal systems compared with hot-water systems. *Economic Geol.* **66**, 75–97.

Young, R. M. 1996 Phase transitions in one-dimensional steady state hydrothermal flows. *J. Geophys. Res.* **101**, 18011–18022.

Zauderer, E. 1983 *Partial Differential Equations of Applied Mathematics*. John Wiley & Sons.

Zemansky, M. W. 1957 *Heat and Thermodynamics*. McGraw-Hill.